OPTIMUM DIAMETER OF A CIRCULATING FLUIDISED BED COMBUSTOR WITH NEGATIVE WALL HEAT FLUX

Baloyi J. [*, 1, 2], Bello-Ochende T. [3] and Meyer J.P. [1]

[*]Author for correspence

[1]Department of Mechanical and Aeronautical Engineering, University of Pretoria, Private Bag X20, Hatfield, Pretoria, 0028, South Africa

[2]Modelling and Digital Science, Council for Scientific and Industrial Research, P.O. Box 395, Pretoria, 0001, South Africa

[3]Department of Mechanical Engineering, University of Cape Town, Private Bag X3, Rondebosch, 7701, South Africa

E-mail: jbaloyi@csir.co.za

ABSTRACT

The focus of the world is the reduction of greenhouse gases like carbon dioxide, which contribute to the global warming currently experienced. Since most of the carbon dioxide emitted into the atmosphere is from fossil fuel combustion, alternative energy source were developed and others are currently under study to see if they can be good alternatives. One of these alternative sources of energy is the combustion of wood instead of coal. Wood has an advantage for being a neutral carbon fuel source, and that currently installed infrastructure used to combust coal can be retrofitted to combust wood or a mixture of wood and coal in an attempt to reduce the carbon dioxide emissions. In this study the effect a change in diameter of a combustor has on irreversibilities in a 7 m circulating fluidised bed combustor with a negative wall heat flux, firing a mixture of air and solid pitch pine wood, was investigated. An analytical expression was derived that predicts the entropy generation rate, thereby the irreversibilities, of a combustor with a negative wall flux as a function of the combustor diameter. A numerical code was used to compute the molar fractions of combustion products needed as an input in the analytical expression. In the numerical code the combustion process was modelled by a non-premixed combustion model, with a P1 radiation model. Simulations were run using a steady Reynolds averaged Navier Stokes model. The analytical expression predicted the optimum diameter that results in minimum irreversibilities to be 0.32 m for a rich mixture with an Air-Fuel mass ratio of 6, and an incoming air temperature of 400 K.

INTRODUCTION

The focus of the world is the reduction of greenhouse gases like carbon dioxide. Since most of the carbon dioxide emitted into the atmosphere is from fossil fuel combustion, alternative energy source were developed and others are currently under study to see if they can make good alternatives. One of these alternative sources of energy is the combustion of wood instead of coal. Wood has an advantage for being a neutral carbon fuel source, and that currently installed infrastructure used to combust coal can be retrofitted to combust wood or a mixture of wood and coal in an attempt to reduce the carbon dioxide emissions

NOMENCLATURE

Symbol	Units	Description
A	[mm^2]	Cross-sectional area
AF	[-]	Air-Fuel mass ratio
B_1	[-]	Equation term
B_3	[-]	Equation term
B_4	[-]	Equation term
B_6	[-]	Equation term
$\bar{c}$	[kJ/kmol.K]	Molar specific heat
c	[kJ/kg.K]	Specific heat
c_p	[kJ/kg.K]	Specific heat at constant pressure
C	[-]	Atomic carbon
C_d	[-]	One of the mixture fraction variance transport equation constant
C_g	[-]	One of the mixture fraction variance transport equation constant
CO	[-]	Carbon monoxide
CO_2	[-]	Carbon dioxide
D	[mm]	Combustor diameter
$\bar{f}$	[-]	Mixture fraction
$\overline{f'^2}$	[-]	Mixture fraction variance
$\vec{F}$	[-]	Body force
g	[m/s^2]	Gravitational acceleration magnitude
$\vec{g}$	[m/s^2]	Gravitational acceleration
G	[kg/s/m^2]	Mixture mass flux
$\bar{h}$	[kJ/kmol]	Specific enthalpy
$\bar{h}^0$	[kJ/kmol]	Enthalpy of formation

Symbol	Units	Description
H	[mm] , [kJ]	Atomic hydrogen; Height; total enthalpy
H_2	[-]	Molecular hydrogen
H_2O	[-]	Water vapour
$\hat{i}$	[-]	Unit vector
$\dot{I}$	[W]	Irreversibility
k	[-]	Turbulent generate rate
L	[mm]	Length
$\dot{m}$	[kg/s]	Mass flow rate
M	[kg/kmol]	Molecular weight
n	[-]	Stoichiometric coefficient
N	[-]	Atomic nitrogen; Entropy generation number
N_2	[-]	Molecular nitrogen
O	[-]	Atomic oxygen
O_2	[-]	Molecular oxygen
P	[Pa]	Pressure
q''	[W/m^2]	Wall heat flux
$\bar{R}$	[kJ/kmol.K]	Universal gas constant
$\bar{s}$	[kJ/kmol.K]	Specific entropy
$\bar{s}^{\circ}$	[kJ/kmol.K]	Absolute entropy
$\dot{S}_{gen}$	[W/K]	Entropy generation rate
S_h	[-]	Viscous dissipation energy source term
S_m	[-]	Solid phase to gas phase mass transfer source term
T	[K]	Temperature
$\vec{v}$	[m/s]	Velocity
x	[-]	Molar fraction
X_1	[-]	Equation term
X_2	[-]	Equation term
X_3	[-]	Equation term
X_4	[-]	Equation term
Y	[-]	Mass fraction

Greek symbols

Symbol	Units	Description
ρ	[kg/m^3]	Density
ε	[-]	Void fraction; turbulent dissipation rate
σ_t	[-]	One of the mixture fraction variance transport equation constant
μ	[Pa.s]	Molecular viscosity
μ_t	[Pa.s]	Turbulent viscosity
$\bar{\bar{\tau}}$	[-]	Stress tensor

Subscripts

Symbol	Units	Description
0	[-]	Superficial
Air	[-]	Air
$char$	[-]	Char
CO	[-]	Carbon monoxide

Symbol	Units	Description
CO_2	[-]	Carbon dioxide
f	[-]	Fuel
g	[-]	Gas
$gen, \min$	[-]	Minimum entropy generation rate
$gen(h)$	[-]	
$gen(p)$	[-]	Entropy generation rate due to frictional pressure drop
H_2	[-]	Molecular hydrogen
H_2O	[-]	Water vapour
$h-t$	[-]	Heat transfer
i	[-]	Counting index
l	[-]	Maximum number of products
m	[-]	Maximum number of reactants; mixture
mf	[-]	Minimum fluidisation
N_2	[-]	Molecular nitrogen
O_2	[-]	Molecular oxygen
p	[-]	Product species
r	[-]	Reactant species
ref	[-]	Environment reference
s	[-]	Solid species
sd	[-]	Dense zone solid species
se	[-]	Exit zone solid species
t	[-]	Total of solid and gas
th	[-]	Theoretical amount of air ratio
w	[-]	Wall

The influence of geometric parameters on the efficiency of energy production has been an area of interest for researchers looking to get the most out of their apparatus used for this purpose. Hua, Wu and Kumar [1] discovered that changing the wall conditions from adiabatic to heat loss through a wall on the combustion chambers has the effect of quenching, even extinguishing the combustion process inside the chamber burning a hydrogen-air mixture, as they vary from millimetre to micro scale size when they were analysed numerically. [2] expanded on the worked done in [1] to optimise the micro-combustor in terms of the best equivalence ratio to operate the micro-combustor at. Norton and Vlachos [3] numerically studied the effects of wall thickness and flow velocities on the combustion characteristics and flame stability in a premixed methane/air mixture micro-burner. They found two modes of flame blowout, one due to thick wall thermal conductivities and another due to low flow velocities. Louis et al [4 found that to compare well with experimental data it is necessary to include the mixing, combustion and heat loss associated with non-adiabatic modelling in accurately predicting the NO formation in flames with heat loss for an air cooled syngas combustion chamber. Li and Zhong [5] experimentally found that for a stainless steel micro-tube burning a methane/oxygen mixture the heat loss due radiation

constituted about 70% of the total heat loss. Feng, Liu and Li [6] found that the higher the axial wall temperature gradient the more stable the flame that can be realised for a given tube size when they numerically studied the combustion of an air-methane mixture inside a small tube. The technique of analysing and minimising the entropy generation rate of a process was demonstrated with good effect in studies by [7-10]. In furtherance of the work done in Baloyi, Bello-Ochende and Meyer [7], Baloyi, Bello-Ochende and Meyer [11] and [12] in this study the effect of a change in diameter of a combustor has on irreversibilities in a 7 m circulating fluidised bed combustor with a negative wall heat flux, firing a mixture of air and solid pitch pine wood, was investigated.

EXERGY ANALYSIS
The irreversibility generation rate that results from the combustion-heat transfer and frictional pressure drop processes taking place in an adiabatic combustor is as given by equation (1) [13-15].

$$\dot{I} = \frac{\dot{m}_f}{M_f}\left(\sum_{i=1}^{m} n_{ri}\left(\overline{h} - T_{ref}\overline{s}\right)_{ri} - \sum_{i=1}^{l} n_{pi}\left(\overline{h} - T_{ref}\overline{s}\right)_{pi}\right)$$
$$-\left(1 - \frac{T_{ref}}{T_w}\right)q''\pi DL$$
(1)

Since the wall temperature, the enthalpy and entropy terms of the combustion products are unkowns for a rich mixture in equation (1), the irreversibility generation rate can also be defined, by equation (2)

$$\dot{I} = T_{ref}\dot{S}_{gen}$$
(2)

Where $\dot{S}_{gen}$ is the entropy generation rate. The specific entropy is given by equation (3).

$$\overline{s}_{pi} = \overline{s}_{pi}^{\circ}(T) - \overline{R}\ln(Px_{pi}/P_{ref})$$
(3)

The static pressure in the combustor is the same as the reference static pressure, i.e. $P = P_{ref}$, and the molar fraction of each product species, x_{pi}, is given by equation (4)

$$x_{pi} = n_{pi}\bigg/\sum_{i=1}^{l} n_{pi}$$
(4)

n_{pi} is the stoichiometric coefficient of combustion product species i. The same expressions apply for reactants. $\overline{h}$ is the specific enthalpy, $\overline{s}_{pi}^{\circ}$ is the absolute entropy, $\overline{R}$ is the universal gas constant, p is the static pressure, P_{ref} is the reference static

pressure of the environment and T_{ref} is the reference temperature of the environment. . The specific entropy of the solid fuel was computed by defining [13] it as given by equation (5).

$$\overline{s} = \overline{c}\ln(T_f/298)$$
(5)

$\overline{c}$ is the molar specific heat of the solid fuel. The study was conducted a combustor with a negative heat flux wall condition burning pitch pine wood, and an incoming air temperature of 400 K as investigated in [11]. The combustor is as illustrated in Fig. 1. The combustor was made out of a cylinder with a negative heat flux wall condition, inlets for the solid fuel and primary air inlet for the air used to devolatilise the solid fuel and secondary air inlets that were needed to complete the combustion of the fuel.
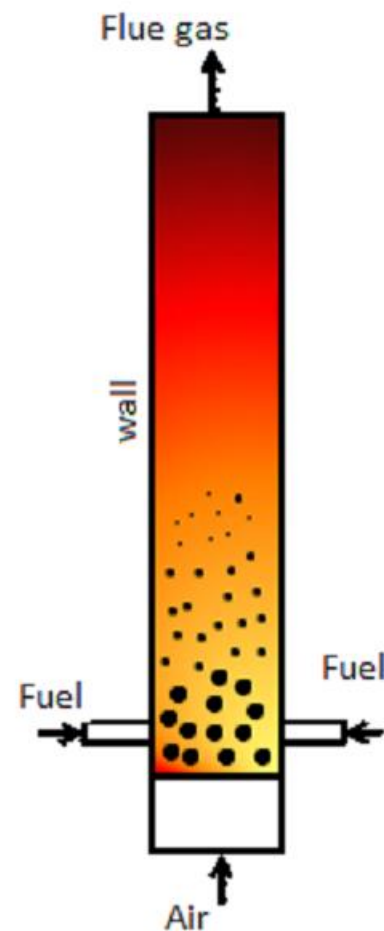
Figure 1 Schematic of a combustor (adapted from [7]).

The air-fuel mass ratio (AF) of 6 was chosen for this study because it was identified in [12] to be the minimum AF for a combustor with a negative heat

flux wall condition of 7500 W/m², and a diameter of 0.3 m as shown in Figure 2.
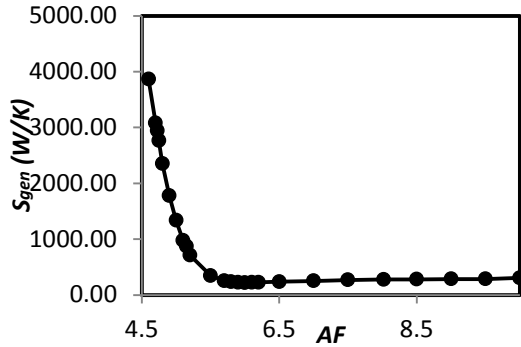
Figure 2 Plots of the variation of entropy generation rate with AF for case with wall heat flux of -7500 W/m².

The chemical formula of the solid fuel as computed in [11] is given by $C_{4.9}H_{7.2}O_2$, the lower heating value of the fuel from [11] was given as 16091.2 kJ/kg and the molecular weight of the fuel was calculated as 98 kg/kmol. The specific heat at constant pressure was also given as 1.680 kJ/kg.K. The entropy generation rate is constituted by the frictional pressure drop and combustion-heat transfer terms [16]. The frictional pressure drop term, due to the air-fuel mixture as it flows through the riser [17], was derived in [7] and is given by equation (6).

$$\dot{S}_{gen(p)} = \dot{m}_f (AF+1)(\rho_f - \rho_g)g \times$$

$$\frac{\left[\dfrac{(\varepsilon_{sd} - \varepsilon_{se})(1 - \varepsilon_{sd})\dot{m}_f AF}{10\rho_g A} + H_t \varepsilon_{sd} + \ln\left(\dfrac{\varepsilon_{se} - \varepsilon_s^*}{\varepsilon_{sd} - \varepsilon_s^*} \right)\left(\dfrac{\varepsilon_{sd} - \varepsilon_s^*}{10\rho_g A} \right)(1 - \varepsilon_{sd})\dot{m}_f AF \right]}{(\varepsilon_{se}\rho_f + (1 - \varepsilon_{se})\rho_g)T_m}$$

$$(6)$$

ΔP is the pressure drop across the combustor, $\dot{m}_f$ is the solid fuel mass flow rate, ρ_m is the mixture density, T_m is the mixture temperature.

The combustion-heat transfer term, due to combustion and/or heat transfer processes, was also derived in [7] and is given by equation (7).

$$\dot{S}_{gen(h)} = \frac{\dot{m}_f}{M_f}\left(\begin{array}{c} \displaystyle\sum_{j=1}^{l} n_{pj}(\bar{s}° - \bar{R}\ln(x))_{Pj} \\ -\displaystyle\sum_{j=1}^{m} n_{rj}(\bar{s}° - \bar{R}\ln(x))_{rj} \\ +\dfrac{\rho_{char}}{\rho_g}n_{char}c_{char}M_{char}\ln\left(T_{char}/298\right) \\ -\dfrac{\rho_f}{\rho_g}n_f c_f M_f \ln\left(T_f/298\right) \end{array} \right)$$

$$(7)$$

A negative wall heat flux of 7500 W/m² was applied over the wall of the combustor, which results in a heat rate of energy extracted through the wall of 48.5 kW$_{th}$. This corresponds to about 20% of the total thermal heat rate of 241 kW$_{th}$ generated in the combustor for a fuel mass flow rate of 0.015 kg/s. The analysis of the entropy generation rate is the same as that of [7] except that there is an additional term due to heat transfer [16] through the wall of the combustor, and this term is as expressed in equation (8).

$$\dot{S}_{gen(h-t)} = -\frac{2\pi LDq''}{T_m + \Delta T} \tag{8}$$

Where L is the length of the combustor, D is the diameter of the combustor, q'' is the wall heat flux and ΔT is the change if temperature across the length of the combustor. The only term that is unknown in equation (8) is ΔT which can be described by equation (9).

$$\Delta T = \frac{q''}{c_p GSt} \tag{9}$$

Where $G = \dot{m}_f (AF+1)/A$ is the mixture mass flux and $St = Nu/Re_D Pr$ is the Stanton number. The Prandtl number Pr is assumed to be 0.69 [18] for the gas species mixture involved in the combustion process and Re_D is the Reynolds number based on the combustor diameter. The Nusselt number [16] is given by equation (10), assuming turbulent internal flow.

$$Nu = 0.023 Re_D^{0.8} Pr^{0.4} \tag{10}$$

Substituting equation (10) into equation (9) and taking all the above into consideration, equation (9) becomes:

$$\Delta T = \frac{\pi D^2 q''}{0.1148 c_p \dot{m}_f (AF + 1) \mathrm{Re}_D^{-0.2}} \quad (11)$$

Substituting equation (11) into equation (8) results in:

$$\dot{S}_{gen(h-t)} = -\frac{0.2296\pi L D c_p \dot{m}_f (AF + 1) q'' \mathrm{Re}_D^{-0.2}}{0.1148 c_p \dot{m}_f (AF + 1) T_m \mathrm{Re}_D^{-0.2} + \pi D^2 q''} \quad (12)$$

When equation (12) is added to equation (7), what results is an equation that describes the entropy generation rate due combustion and heat transfer through a wall for the combustor with a heat flux wall condition, as expressed by equation (13).

$$\dot{S}_{gen} = \frac{\dot{m}_f}{M_f} \left(\begin{array}{l} \sum_{j=1}^{l} n_{pj} \left(\bar{s}^{\circ} - \bar{R} \ln(x) \right)_{Pj} \\ - \sum_{j=1}^{m} n_{rj} \left(\bar{s}^{\circ} - \bar{R} \ln(x) \right)_{rj} \\ + \frac{\rho_{char}}{\rho_g} n_{char} c_{char} M_{char} \ln\left(T_{char}/298 \right) \\ - \frac{\rho_f}{\rho_g} n_f c_f M_f \ln\left(T_f/298 \right) \end{array} \right)$$
$$- \frac{0.2296\pi L D c_p \dot{m}_f (AF + 1) q'' \mathrm{Re}_D^{-0.2}}{0.1148 c_p \dot{m}_f (AF + 1) T_m \mathrm{Re}_D^{-0.2} + \pi D^2 q''} \quad (13)$$

Where the Reynolds number is as expressed by equation (14).

$$\mathrm{Re}_D = \frac{4\dot{m}_f (AF + 1)}{\pi \mu D} \quad (14)$$

Where μ is the mixture dynamic viscosity.

When taking the all the terms that constitute the entropy generation rate into account by adding equation (13) with equation (6), the total entropy generation rate is expressed by equation (15).

$$\dot{S}_{gen} = B_1 \left[\frac{X_1}{\pi D^2} + B_3 + \frac{4 X_2}{\pi D^2} \right] + B_4$$
$$- \frac{X_3 D \mathrm{Re}_D^{-0.2}}{B_6 \mathrm{Re}_D^{-0.2} + X_4 D^2} \quad (15)$$

Where

$$B_1 = \frac{\dot{m}_f (AF + 1)(\rho_f - \rho_g) g}{\left[\varepsilon_{se} \rho_f + (1 - \varepsilon_{se}) \rho_g \right] T_m} \quad (16)$$

$$B_3 = H_t \varepsilon_{sd} \quad (17)$$

$$B_4 = \dot{S}_{gen(h)} =$$
$$\frac{\dot{m}_f}{M_f} \left(\begin{array}{l} \sum_{j=1}^{l} n_{pj} \left(\bar{s}^{\circ} - \bar{R} \ln(x) \right)_{Pj} \\ - \sum_{j=1}^{m} n_{rj} \left(\bar{s}^{\circ} - \bar{R} \ln(x) \right)_{rj} \\ + \frac{\rho_{char}}{\rho_g} n_{char} c_{char} M_{char} \ln\left(T_{char}/298 \right) \\ - \frac{\rho_f}{\rho_g} n_f c_f M_f \ln\left(T_f/298 \right) \end{array} \right)$$
$$(18)$$

$$B_6 = 0.1148 c_p \dot{m}_f (AF + 1) T_m \quad (19)$$

$$X_1 = \frac{(\varepsilon_{sd} - \varepsilon_{se})(1 - \varepsilon_{sd}) \dot{m}_f AF}{10 \rho_g} \quad (20)$$

$$X_2 = \frac{\dot{m}_f AF}{10 \rho_g} \ln\left(\frac{\varepsilon_{se} - \varepsilon_s^*}{\varepsilon_{sd} - \varepsilon_s^*} \right)(\varepsilon_{sd} - \varepsilon_s^*)(1 - \varepsilon_{sd}) \quad (21)$$

$$X_3 = 0.2296\pi L c_p \dot{m}_f (AF + 1) q'' \quad (22)$$

$$X_4 = \pi q'' \quad (23)$$

The entropy generation rate in equation (15) can be expressed as a function of Reynolds number as given by equation (24).

$$\dot{S}_{gen} = \left[\frac{\pi B_1 X_1 \mu^2}{4\dot{m}_f^2 (AF + 1)^2} + \frac{\pi B_1 X_2 \mu^2}{4\dot{m}_f^2 (AF + 1)^2} \right] \mathrm{Re}_D^2$$
$$+ B_1 B_3 + B_4 - \frac{4\pi \mu X_3 \dot{m}_f (AF + 1) \mathrm{Re}_D^{0.8}}{\pi^2 \mu^2 B_6 \mathrm{Re}_D^{1.8} + 16 X_4 \dot{m}_f^2 (AF + 1)^2} \quad (24)$$

The entropy generation number, N_s [7] which is the quotient of the entropy generation rate at any Reynolds number and the minimum entropy generation rate, was used to analyse the penalty paid by running the combustor at a Reynolds

number other than the optimum and is as given by equation (25).

$$N_s = \frac{\dot{S}_{gen}}{\dot{S}_{gen,min}} \qquad (25)$$

NUMERICAL MODEL

The combustor produced 241 kW$_{th}$ when complete combustion of pitch pine wood occurs with theoretical amount of air. The combustor had a diameter of 300 mm and a height of 7000 mm as illustrated in Fig. 3.
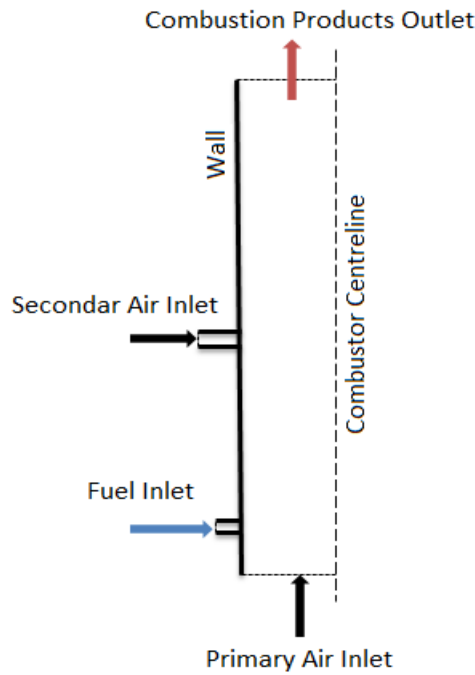
Figure 3 Schematic of the combustor showing boundary placements (adapted from [7]).

The mass flow rate of the incoming solid fuel was fixed at a value of 0.015 kg/s so as to have a common maximum heat generation rate of 241 kW$_{th}$ since the lower heating value is fixed and unique for any particular fuel. ANSYS Fluent 14 [19] was used to simulate the combustion process inside the combustor. The combustion process was modelled using the non-premixed combustion model because the solid fuel is only specified in ultimate analysis data [20] as given in Table 2, and the combustion model gives an option of specifying the fuel as an empirical stream. The inlet diffusion option was selected.

Table 1 Pitch pine ultimate analysis data (adapted from [19]).

Element	Value
C	59.0 (%)
H	7.2 (%)
O	32.7 (%)
Ash	1.13 (%)
HHV	24220 (kJ/kg)
LHV	16091.2 (kJ/kg)
Molecular weight	98 (kg/kmol)

The continuity and momentum equations [19] as expressed by equation (26) and equation (28) respectively were solved for under steady state condition.

$$\nabla \cdot (\rho \vec{v} \overline{f}) = \nabla \cdot \left(\frac{\mu_t}{\sigma_t} \nabla \overline{f} \right) + s_m \qquad (26)$$

$$\nabla \cdot (\rho \vec{v} \overline{f'^2}) = \nabla \cdot \left(\frac{\mu_t}{\sigma_t} \nabla \overline{f'^2} \right) + C_g \mu_t (\nabla \overline{f})^2 - C_d \rho \frac{\varepsilon}{k} \overline{f'^2} \qquad (27)$$

$$\nabla \cdot (\rho \vec{v} \vec{v}) = -\nabla p + \nabla \cdot (\overline{\overline{\tau}}) + \rho \vec{g} + \vec{F} \qquad (28)$$

The stress tensor [19] is given by equation (29).

$$\overline{\overline{\tau}} = \mu \left[(\nabla \vec{v} + \nabla \vec{v}^T) - \frac{2}{3} \nabla \cdot \vec{v} \hat{i} \right] \qquad (29)$$

μ is the molecular viscosity of the continuous phase, $\vec{F}$ is the interactive body forces between the dispersed and the continuous phases, S_m is the source term accounting for the mass transfer from the solid phase to the gas phase and $\hat{i}$ is a unit vector. $\overline{f}$ and $\overline{f'^2}$ are the mixture fraction and its variance, and are computed by applying an assumed shape probability density function (β-function) when modelling the turbulence-chemistry interaction.

The energy for the non-premixed combustion model [19] was as expressed by equation (30).

$$\nabla \cdot (\rho \vec{v} H) = \nabla \cdot \left(\frac{k_t}{c_p} \nabla H \right) + S_h \qquad (30)$$

The total enthalpy H is given by equation (31).

$$H = \sum_{j=1}^{m} Y_j \int_{T_{ref,j}}^{T} \left(c_{p,j} dT + h_j^0 (T_{ref,j}) \right) \qquad (31)$$

Y_j is the mass fraction, $c_{p,j}$ is the specific heat and constant pressure and $h_j^0(T_{ref,j})$ is the enthalpy of

formation of the jth species. S_h is the source term due to viscous dissipation. The use of the chosen combustion model required the use of a turbulent model because the combustion model is a mixture model. To this end the $k - \varepsilon$ turbulent model with enhanced wall function option was chosen for all simulations.

The combustor had four mass flow inlets for the solid fuel as shown in Figure 4, each with equal mass flow rate of 0.00375 kg/s. The inlet temperature of the fuel at each inlet was set at 600K. The temperature value was selected to be same as the devolatilisation temperature of pitch pine [20]. The oxidising air was split into the primary and secondary air, each making up half of the total air used in the oxidation of the fuel. The reason for splitting the oxidising air was to enable the modelling of incomplete combustion to take place. The primary air entered the combustor at the base with a single fixed mass inlet, with half of the total air mass flow rate. The secondary air four fixed mass inlets were situated a quarter of the height up the combustor, each having an eighth of the total air mass flow rate. The inlet temperature at all eight air inlets was set at 400K. The wall boundar condition of the combustor was a negative heat flux of 7500 W/m^2. The data that was extracted from the simulations were the temperature at the pressure outlet boundary and the combustion products molar fractions. Figure 4 shows the placement and types of boundaries applied on the combustor.
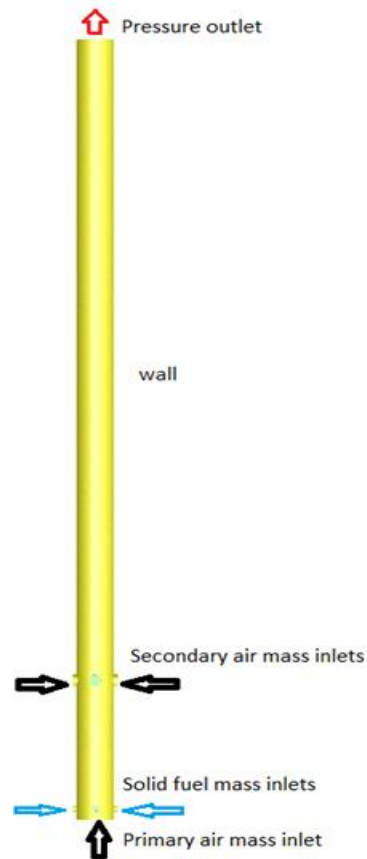
Figure 4   Schematic of the geometry used in Ansys Fluent 14 to model the combustor.

The mesh used for the numerical simulations aried from 750000 to 850000 unstructured polyhedral cells. The Presto scheme was used to solve for pressure and second-order upwind schemes were used to solve for the continuity, energy, turbulence and mass fraction. The results obtained when using equation (6) and equation (7) to process data from numerical simulations and data from thermodynamics tables data [13] were compared for the case of complete combustion with varying amount of excess air, that is lean mixtures. It was found that the results from numerical simulations data compared well with results from thermodynamics tables data as shown in Figure 5.
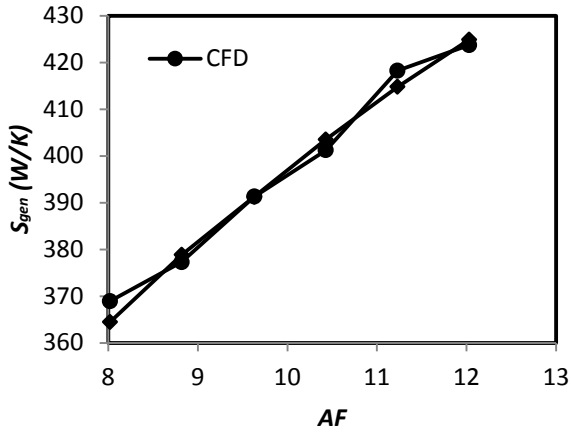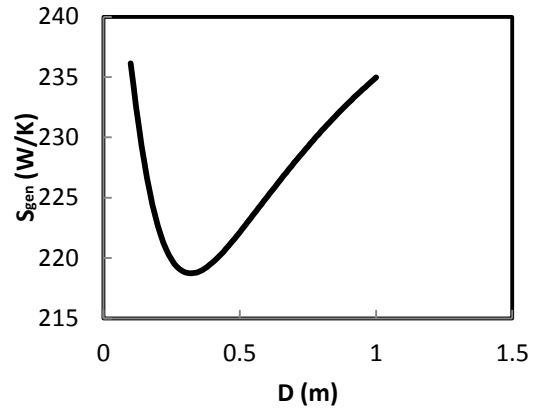
Figure 5 The entropy generation rate profile as a function of AF in an adiabatic combustor for lean mixtures.

RESULTS AND DISCUSSION

The molar fractions of combustion products were incorporated into equation (24) in order to compute the entropy generation rate of the combustor. The computed entropy generation rate for a wide range of Reynolds number based on the combustor diameter was plotted in Figure 6. The figure shows that the minimum entropy generation rate of about 218 W/K occurred at a Reynolds number of about 25000. This Reynolds number corresponds to a combustor diameter of 0.32 m as shown by Figure 7. Since the AF has been fixed at a value of 6, the entropy generation rate term due to combustion remains constant even when the there is a change in combustor diameter. Also given that the contribution of the pressure loss term is negligible as discovered in [7], therefore all the change in entropy generation rate is all due to the heat transfer term through the wall of the combustor. This means that the optimum diameter discovered in this study is unique for a combustor run at an AF of 6.
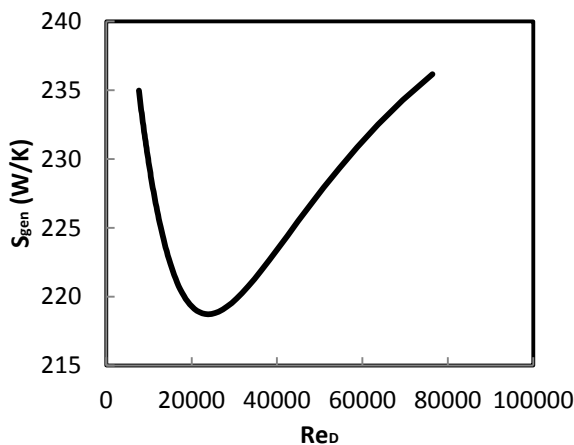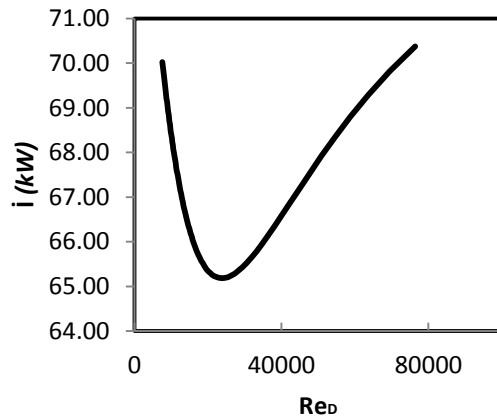

Figure 6 The entropy generation rate profile as a function of Re_D in a combustor ran at an AF of 6.

Figure 7 The entropy generation rate profile as a function of combustor diameter in a combustor ran at an AF of 6.

The corresponding irreversibilities rate was also computed, and is shown in Figure 8.

Figure 8 The irreversibilities rate profile as a function of Re_D in a combustor ran at an AF of 6.

The penalty that is paid when a combustor has a diameter that is not 0.32 was also computed as represented by N_s as can be seen in Figure 9. The figure shows that at diameters of 0.1 m and 0.97 the penalty paid was an extra 7% in entropy generation rate.
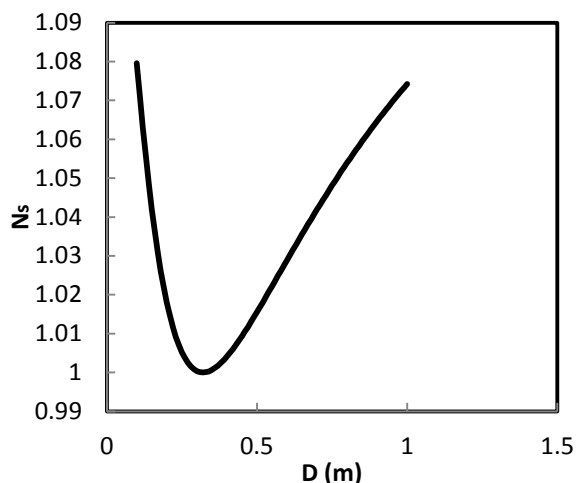
Figure 9   The entropy generation number profile as a function of combustor diameter in a combustor ran at an AF of 6.

CONCLUSIONS

The combustor with a negative heat flux wall condition was simulated at an AF of 6 for varying combustor diameters to find the diameter with the minimum entropy generation rate. It was discovered that a diameter of 0.32 m resulted in the minimum entropy generation rate. It was also discovered that the penalty paid, when a combustor with a diameter of 0.1 m or 0.97 m was used, was 7%

REFERENCES

[1] Hua J, Wu M, Kumar K. Numerical simulation of the combustion of hydrogen-air mixture in micro-scaled chambers. Part I: Fundamental study. Chemical Engineering science 2005; 60: 3497-3506.
[2] Hua J, Wu M, Kumar K. Numerical simulation of the combustion of hydrogen-air mixture in micro-scaled chambers. Part II: CFD analysis for a micro-combustor. Chemical Engineering science 2005; 60: 3507-3515.
[3] Norton DG, Vlachos DG. Combustion characteristics and flame stability at the microscale: a CFD study of premixed methane/air mixtures.
Chemical Engineering science 2003; 58: 4871-4882.
[4] Louis JJJ, Kok JBW, Klein SA. Modeling and measurements of a 16-kW turbulent nonadiabatic syngas diffusion flame in a cooled cylindrical combustion chamber. Combustion and Flame 2001; 125: 1012-1031.
[5] Li J, Zhong B. Experimental investigation on heat loss and combustion in methane/oxygen micro-tube combustor. Applied Thermal Engineering 2008; 28: 707-716.
[6] Feng L, Liu Z, Li Y. Numerical study of methane and air combustion inside a small tube with an axial temperature gradient at the wall. Applied Thermal Engineering 2010; 30: 2804-2807.
[7] Baloyi J, Bello-Ochende T, Meyer JP. Thermodynamic optimisation and computational analysis of irreversibilites in a small-scale wood-fired circulating fluidised bed adiabatic combustor. Energy 2014; 70: 653-663.
[8] Le roux WG, Bello-Ochende T, Meyer JP. Optimum performance of a small-scale open and direct solar thermal Brayton cycle at various environmental conditions and constraints. Energy 2012; 46 (1): 42-50.
[9] Mwesigye A, Bello-Ochende T, Meyer JP. Numerical investigation of entropy generation in a parabolic through receiver at different concentration ratios. Energy 2013; 53: 114-127.
[10] Le Roux WG, Bello-Ochende T, Meyer JP. Operating conditions of an open and direct solar thermal Bryaton cycle with optimised cavity receiver and recuperator. Energy 2011; 36 (10): 6027-6-36.
[11] Baloyi J, Bello-Ochende T, Meyer JP. "The analysis of exergy destruction of a wood fired adiabatic combustor". International Conference on Applied Energy. Pretoria, South Africa, 2013.
[12] Baloyi J, Bello-Ochende T, Meyer JP." Wall heat flux and air inlet temperature influences on the thermodynamic optimisation of irreversibilities of a small scale circulating fluidised bed combustor". manuscript, 2015.
[13] Moran MJ, Shapiro HN. Fundamentals of engineering thermodynamics. 3rd Ed., SI Version, John Wiley and Sons Inc.: Chichester, 1998.
[14] Anamalai K, Puri K. Advanced thermodynamics engineering. CRC Press Inc.: Florida, 2002.
[15] Bejan A. Advanced engineering thermodynamics. John Wiley and Sons Inc.: New York, 1988.
[16] Bejan A. Entropy generation minimization: The method of thermodynamic optimization of finite-size systems and finite-time processes. CRC Press Inc.: Florida, 1996.
[17] Kunii D, Levenspiel O. Fluidization Engineering. Stoneham: Massachusetts, 1991.

[18] White FM. Viscous Fluid Flow. 3rd Ed., International Edition. McGraw-Hill: Singapore, 2006.

[19] ANSYS FLUENT Release 14.0. Theory Guide. ANSYS Inc.: Southpointe, 2011.

[20] Tillman DA, Rossi AJ, Kitto WD. Wood Combustion: Principles, Processes and Economics. Academic Press Inc.: New York, 1981.